Solvation Models for the Excited-States of a Rhenium Diimine Carbonyl Complex: A Methodological Comparative Study

Sebastian Mai [1], Hugo Gattuso [2,3], Maria Fumanal [4], Aurora Muñoz-Losa*[1], Antonio Monari †[2,3], Chantal Daniel ‡[4] and Leticia González §[1]

[1]Institute of Theoretical Chemistry, Faculty of Chemistry, University of Vienna, Währinger Straße 17, Vienna, 1090 Austria.
[2]Université de Lorraine Nancy, Theory-Modeling-Simulation SRSMC, Boulevard des Aiguillettes, Vandoeuvre-lès-Nancy, 54500 France.
[3]CNRS, Theory-Modeling-Simulation SRSMC, Boulevard des Aiguillettes, Vandoeuvre-lès-Nancy, 54500 France.
[4]Laboratoire de Chimie Quantique, Institut de Chimie Strasbourg, UMR-7177 CNRS/Université de Strasbourg, 1 Rue Blaise Pascal BP 296/R8, Strasbourg, 67008 France.

Molecular Dynamics

Definition of Imidazole Torsion Angle

We use the following definition of the torsion angle for the imidazole (Im) ligand of $[Re(Im)(CO)_3(Phen)]^+$ (see Figure S1 for definition of the dihedrals Φ_1 and Φ_2):

$$\Theta = \frac{\Phi_1 + \Phi_2}{2} + \begin{cases} -90 & \text{, if } \Phi_1 < \Phi_2 \\ 90 & \text{, else} \end{cases} \tag{1}$$

If the torsion angle Θ is not in the interval from $-180°$ to $180°$, it is shifted by $\pm 360°$ accordingly. With this definition, conformer A is at $-90°$, A′ is at $+90°$, and conformer B is at approximately $0°$ and $\pm 180°$.

Comparison of Force Field versus QM/MM

Figure S2 compares the internal coordinate distribution produced by the classical MD trajectory against a QM/MM trajectory.

The QM/MM trajectory was computed with AMBER17[1] and B3LYP/def2-TZVP (ZORA, RIJCOSX,[2] def-SD ECP on Re) within Orca.[3] The system consisted of the complex and a chloride ion in a cubic box of TIP3P water (802 molecules), where the water was minimized for 7000 and 20000 (steepest descent and conjugate gradient, respectively) around the optimized complex geometry. The system was thermalized in the NVT ensemble for 20 ps (solute atoms restrained with 20 kcal/mol/Å^2), using the weak-coupled algorithm,[4] SHAKE[5], and the particle-mesh Ewald scheme.[6] Equilibration was performed for 1 ps (NPT) and the production run lasted for 2 ps.

Since the QM/MM trajectory is very short, it is not able to accurately reproduce the distribution for slow degrees of freedom, like the Im torsion or the relative motion of Im and Phen. However, for fast

*Present Address: Área de Química Física, University of Extremadura, Avda. Elvas s/n, Badajoz, 06006 Spain.
†antonio.monari@univ-lorraine.fr
‡c.daniel@unistra.fr
§leticia.gonzalez@univie.ac.at

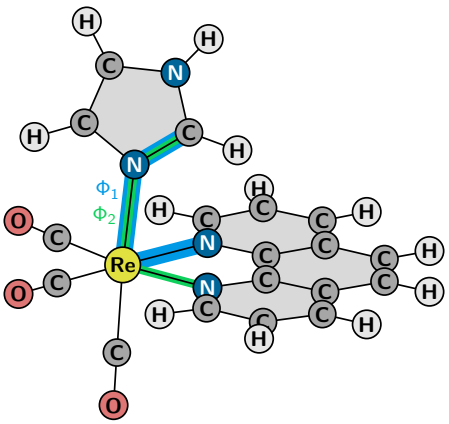

Figure S1: Definition of the dihedral angles Φ_1 and Φ_2. The first atom in the dihedral definition is in both cases the carbon atom. See equation (1) for a definition of the torsion angle Θ.

degrees of freedom—bond lengths and bond angles—it can provide reference data to scrutinize the MD force field.

The histograms in Figure S2 show that the relevant bond parameters are accurately reproduced. Especially the newly parametrized bonds involving the Re atom (bond lengths in panels (a) – (d) of Figure S2, angles in panels (e) – (j)) agree very well with the QM/MM data. The bond lengths of the Phen ligand (panels (k) – (s))—which have a significant effect on the π^* orbitals involved in the MLCT and IL transitions—are also mostly accurate. Some of these bond lengths (e.g., panels (k), (r), and (s)) show slightly larger deviations, which are due to the fact that for Phen the generalized Amber force field was used instead of a custom parametrization. In panel (v), it can be seen that the QM/MM trajectory is clearly too short to reproduce the distribution of the Im torsion angle Θ.

Temporal Evolution of Torsion Angle

Figure S3 shows the temporal evolution of the torsion angle Θ along the MD trajectory. As can be see, the torsion occurs rapidly, faster than the intervals between the data points in the figure (20 ps). This is in agreement with the very small activation barriers of approximately 1 kcal/mol (see the torsion scan in the main manuscript).

Vertical Excitation Spectrum

In Table S1, we present the vertical excitation data for the three minima of [Re(Im)$(CO)_3$(Phen)]$^+$, as shown as part of Figure 4 in the main manuscript. Conformer A here refers to a Θ of -90° (C_s symmetry, with the Im N-H over the phenanthroline), conformer B refers to a Θ of approximately 0° (no symmetry, Im parallel to phenanthroline, enantiomer at $\Theta \approx \pm 180°$), and conformer A′ to a Θ of +90° (C_s symmetry, with the Im N-H over the carbonyls). Table S1 also presents the relevant data for the first 30 triplet states, as well as the state characters of singlets and triplets.

Spin-Orbit Correlation Diagrams

In Figure S4, we show the full spin-orbit mixing correlation diagram, up to an energy of 5.5 eV. Like the truncated correlation diagram in the main manuscript, it can be seen that at the four different geometries, the excitation energies and spin-orbit mixing patterns are quite different.

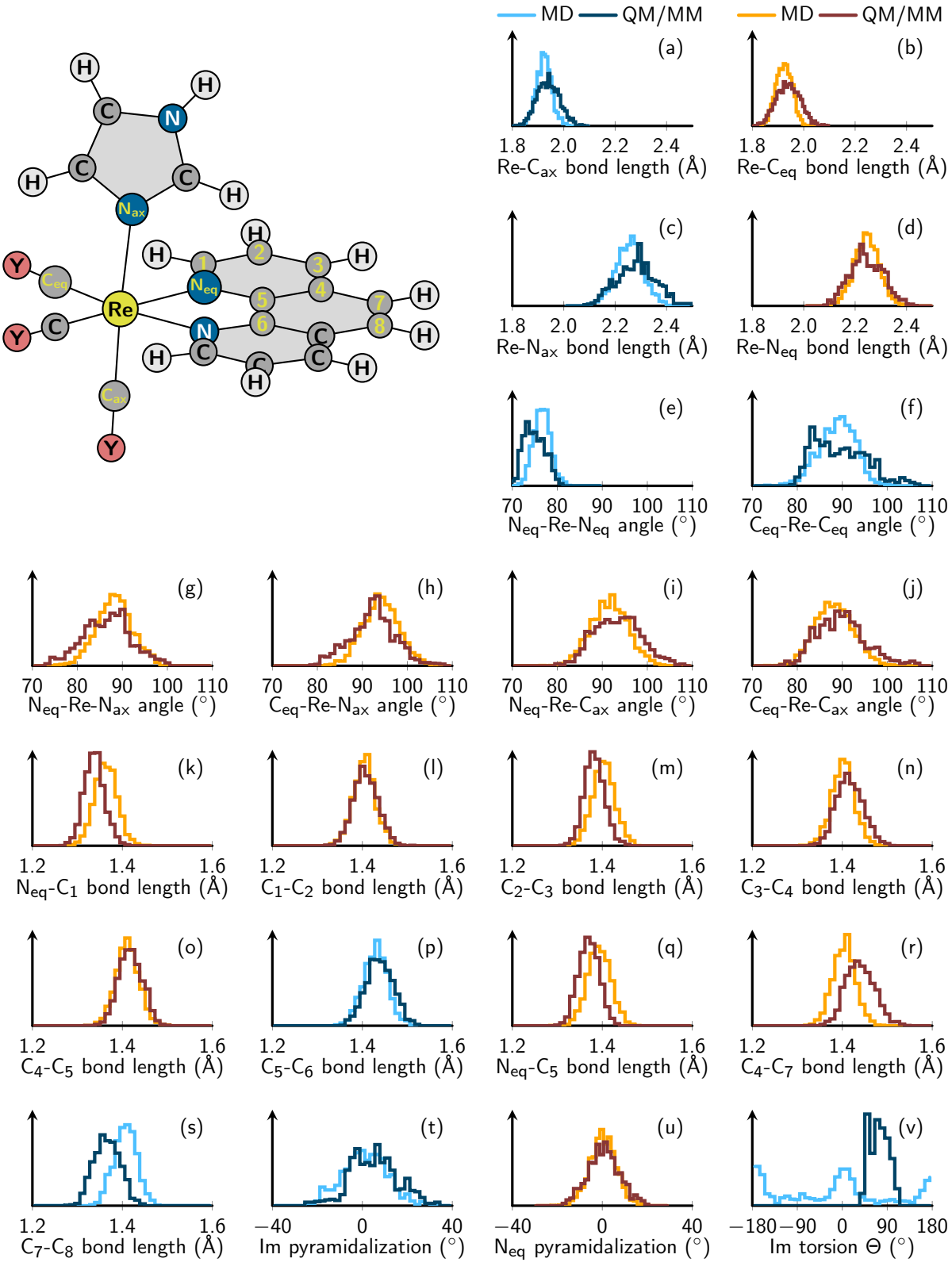

Figure S2: Comparison of internal coordinates from the classical MD and from a 2 ps QM/MM trajectory. Each plots shows the histograms for the internal coordinate given in the axis label. The graph on the upper left shows the relevant atoms marked in yellow. Note that for internal coordinates with a symmetry equivalent (panels (b), (d), (g)–(o), (q), (r), (u); these plots are highlighted in orange/red), the histogram shows the average over the two equivalent internal coordinates.

Table S1: Vertical excitation energies and oscillator strength at the S_0 minimum geometries. Geometries and excitations calculated at the B3LYP/TZP+COSMO level of theory. A linear interpolation scan between these points is given in Figure 4 in the main manuscript.

State	— Conformer A ($\Theta = -90°$) —			— Conformer B ($\Theta \approx 0°$) —			— Conformer A′ ($\Theta = +90°$) —		
	E_{vert} (eV)	f_{osc}	Character	E_{vert} (eV)	f_{osc}	Character	E_{vert} (eV)	f_{osc}	Character
S_1	3.17	0.002	MLCT	3.34	0.094	MLCT	3.14	0.002	MLCT
S_2	3.43	0.070	MLCT	3.34	0.017	MLCT	3.43	0.051	MLCT
S_3	3.51	0.003	MLCT	3.53	0.001	MLCT	3.51	0.000	MLCT
S_4	3.61	0.108	MLCT	3.66	0.022	MLCT	3.60	0.133	MLCT
S_5	3.80	0.024	MLCT	3.71	0.039	MLCT	3.81	0.024	MLCT
S_6	3.88	0.002	LLCT	3.90	0.030	LLCT	3.91	0.001	LLCT
S_7	3.93	0.003	MLCT	3.93	0.000	MLCT	3.94	0.002	MLCT
S_8	4.02	0.000	IL	4.04	0.002	IL	4.03	0.000	IL
S_9	4.24	0.011	LLCT	4.19	0.001	IL/LLCT	4.26	0.028	MC
S_{10}	4.27	0.005	IL	4.20	0.000	MC	4.27	0.005	LLCT
S_{11}	4.28	0.033	MC	4.28	0.003	IL/LLCT	4.27	0.005	IL
S_{12}	4.32	0.000	MC	4.37	0.006	MC	4.34	0.000	MC
S_{13}	4.39	0.000	MC	4.50	0.001	MC	4.37	0.000	MC
S_{14}	4.64	0.175	MLCT/IL	4.61	0.110	IL	4.62	0.145	MC/MLCT/IL
S_{15}	4.64	0.128	IL	4.68	0.344	IL	4.64	0.131	IL
S_{16}	4.75	0.001	MC	4.75	0.006	MC	4.74	0.001	MC
S_{17}	4.82	0.214	MC/MLCT/IL	4.81	0.009	MC/MLCT/IL	4.81	0.302	MC/MLCT/IL
S_{18}	4.87	0.011	MC/IL	4.86	0.021	MC/MLCT	4.86	0.014	MC/IL
S_{19}	4.92	0.544	MC/IL	4.91	0.037	MC/MLCT	4.93	0.500	MC/IL
S_{20}	5.02	0.002	MLCT	4.98	0.550	MC/MLCT/IL	5.03	0.003	MLCT
S_{21}	5.13	0.000	MLCT	5.10	0.007	MLCT	5.14	0.000	MLCT
S_{22}	5.23	0.002	LMCT	5.23	0.001	LMCT	5.25	0.030	MLCT/LMCT
S_{23}	5.29	0.033	LLCT	5.29	0.020	MC	5.32	0.008	LM
S_{24}	5.32	0.001	MC	5.33	0.001	LLCT	5.33	0.005	LMCT/LLCT
S_{25}	5.34	0.049	MLCT	5.35	0.002	LMCT	5.34	0.000	MC
S_{26}	5.36	0.000	LMCT	5.38	0.004	MC/MLCT	5.38	0.000	MC/LMCT
S_{27}	5.42	0.003	MC/IL/LLCT	5.39	0.014	MC/MLCT	5.40	0.001	MC/MLCT/LMCT
S_{28}	5.44	0.005	MC/IL/LLCT	5.42	0.003	MC/MLCT	5.42	0.004	MLCT/IL/LLCT
S_{29}	5.45	0.005	MLCT	5.45	0.004	MLCT/IL/LLCT	5.43	0.002	MC/MLCT/IL
S_{30}	5.55	0.109	MC/MLCT/LMCT	5.54	0.018	MC/MLCT/IL	5.51	0.022	MC/MLCT
T_1	3.01	–	MLCT/IL	3.04	–	MLCT/IL	2.99	–	MLCT/IL
T_2	3.08	–	MLCT/IL	3.08	–	MLCT/IL	3.09	–	MLCT/IL
T_3	3.25	–	IL	3.29	–	MLCT/IL	3.25	–	IL
T_4	3.45	–	MLCT	3.46	–	MLCT/IL	3.46	–	MLCT
T_5	3.51	–	MLCT	3.50	–	MLCT	3.48	–	MLCT
T_6	3.56	–	IL	3.61	–	IL	3.58	–	IL
T_7	3.59	–	MLCT/IL	3.63	–	MLCT/IL	3.59	–	MLCT/IL
T_8	3.85	–	MLCT	3.74	–	MLCT/IL	3.86	–	MLCT
T_9	3.88	–	MC	3.90	–	LLCT	3.88	–	MC
T_{10}	3.88	–	LLCT	3.90	–	IL	3.90	–	IL
T_{11}	3.89	–	LC	3.93	–	MLCT	3.90	–	LLCT
T_{12}	3.94	–	MLCT	3.99	–	MC	3.95	–	MLCT
T_{13}	4.08	–	MC	4.04	–	MC	4.08	–	MC
T_{14}	4.15	–	MC	4.10	–	MC	4.15	–	MC
T_{15}	4.22	–	LLCT	4.21	–	MC	4.25	–	MC
T_{16}	4.25	–	MC	4.23	–	LLCT	4.26	–	LLCT
T_{17}	4.30	–	MC	4.34	–	MC	4.30	–	MC
T_{18}	4.51	–	IL	4.47	–	IL	4.50	–	IL
T_{19}	4.59	–	MC	4.61	–	MC	4.58	–	MC
T_{20}	4.64	–	MLCT/IL	4.65	–	IL	4.61	–	MLCT/IL
T_{21}	4.70	–	IL	4.68	–	IL	4.66	–	IL
T_{22}	4.75	–	IL	4.74	–	IL	4.75	–	IL
T_{23}	4.76	–	IL	4.82	–	MLCT/IL	4.77	–	IL
T_{24}	4.84	–	IL	4.88	–	MLCT/IL	4.84	–	IL
T_{25}	4.92	–	MC	4.92	–	MC/MLCT/IL	4.91	–	IL
T_{26}	4.97	–	MC	5.01	–	MC/MLCT/IL	4.97	–	MC
T_{27}	5.05	–	MLCT	5.04	–	MC	5.06	–	MC
T_{28}	5.11	–	MC	5.04	–	MC	5.07	–	MLCT
T_{29}	5.12	–	LC	5.08	–	MLCT	5.09	–	IL/LMCT
T_{30}	5.15	–	MLCT	5.15	–	MC	5.14	–	MLCT/IL

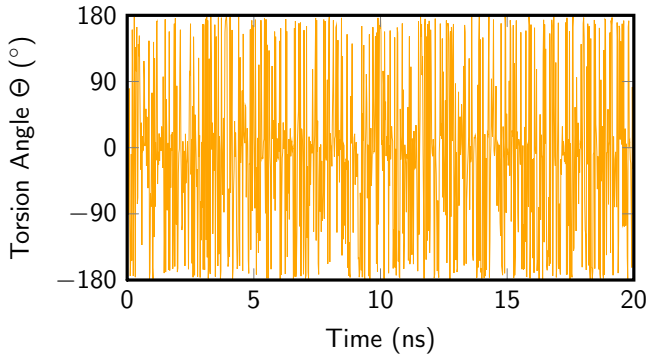

Figure S3: Temporal evolution of the Im torsion angle Θ in the MD trajectory.

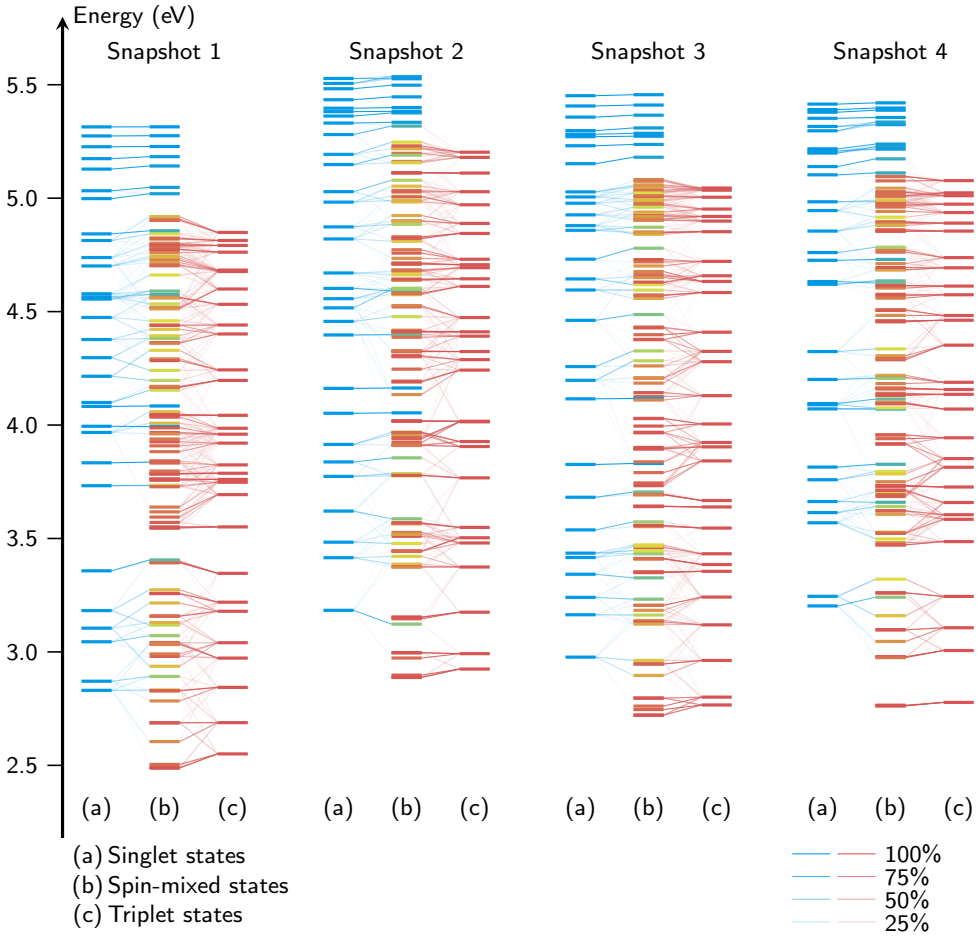

Figure S4: Spin-orbit mixing correlation diagrams of the excited states for four arbitrary MD snapshots, up to an energy of 5.5 eV. For each snapshot, the singlet states are given on the left, the triplets on the right, and the spin-orbit mixed state in the center, with the coloring indicating the total spin expectation value. The thin diagonal lines indicate the contributions of the pure states, with stronger lines indicating a stronger contribution. The vertical axis represents the excitation energy.

Optimized Geometries

The following coordinates of the conformers of $[Re(Im)(CO)_3(Phen)]^+$ were optimized with B3LYP/TZP and COSMO.

```
38
Comformer A (-11.278751 Hartree)
Re +0.000000 +0.000000 +0.000000
N +2.220010 +0.000000 +0.000000
N +0.184410 +0.000000 -2.201110
N +0.184410 -2.129600 -0.556480
N +4.320330 -0.376610 -0.487670
C +3.045890 -0.635360 -0.822720
C -1.928760 -0.057350 -0.074260
C -0.053800 -0.251120 +1.912090
C -0.053800 +1.913460 +0.240440
C +0.211250 +1.067200 -2.996440
C +0.318910 +0.965910 -4.388010
C +0.402390 -0.275380 -4.974080
C +0.382800 -1.425200 -4.161770
C +0.270580 -1.237110 -2.770470
C +0.270580 -2.367710 -1.897340
C +0.382800 -3.666250 -2.431080
C +0.402410 -4.742860 -1.523980
C +0.318930 -4.489650 -0.174840
C +0.211250 -3.168910 +0.274980
C +0.480500 -2.756240 -4.679810
C +0.480480 -3.830940 -3.849850
C +4.326640 +0.463620 +0.600330
C +3.017620 +0.693690 +0.898240
O -3.085550 -0.094340 -0.122160
O -0.075300 -0.428700 +3.057220
O -0.075300 +3.066290 +0.358130
H +0.143690 +2.031830 -2.516580
H +0.335960 +1.869880 -4.979390
H +0.335990 -5.290360 +0.550250
H +0.143690 -2.948500 +1.329580
H +0.560840 -2.885570 -5.751270
H +0.560830 -4.834890 -4.245860
H +0.487180 -0.379790 -6.047840
H +0.487200 -5.755340 -1.896450
H +5.131800 -0.742910 -0.961970
H +2.593100 +1.297350 +1.679900
H +2.766280 -1.269070 -1.643280
H +5.236750 +0.813030 +1.052780
```

```
38
Conformer B (-11.280001 Hartree)
Re +0.000000 +0.000000 +0.000000
N +2.218880 +0.000000 +0.000000
N +0.288680 +0.000000 -2.188330
N +0.331050 -2.118920 -0.520800
N +4.295210 +0.426200 -0.540870
C +3.012290 +0.775210 -0.729370
C -1.922860 -0.124850 -0.134420
C -0.101700 -0.231300 +1.913080
C -0.113360 +1.912610 +0.224170
C +0.234460 +1.052230 -3.003110
C +0.524140 +0.962380 -4.368550
C +0.881150 -0.252480 -4.906340
C +0.938600 -1.386320 -4.074680
C +0.627590 -1.212340 -2.711880
C +0.654310 -2.333990 -1.827470
C +1.000380 -3.607250 -2.320340
C +1.005830 -4.679610 -1.408870
C +0.668210 -4.451020 -0.095060
C +0.334800 -3.155900 +0.314270
C +1.294310 -2.689740 -4.548500
C +1.326240 -3.754260 -3.706890
C +4.339730 -0.620470 +0.349550
C +3.044190 -0.879780 +0.682620
O -3.074570 -0.208780 -0.224360
O -0.154820 -0.397170 +3.059020
O -0.163760 +3.065850 +0.329720
H -0.042890 +1.996130 -2.557850
H +0.466310 +1.853140 -4.977090
H +0.658840 -5.250030 +0.632020
H +0.069510 -2.952350 +1.341110
H +1.537020 -2.806840 -5.596630
H +1.595620 -4.737490 -4.069870
H +1.116570 -0.348080 -5.958250
H +1.273060 -5.670950 -1.750530
H +5.088250 +0.863890 -0.985040
H +2.651440 -1.625680 +1.349450
H +2.694800 +1.566480 -1.383580
H +5.263430 -1.075680 +0.657490
```

```
38
Conformer A' (-11.278791 Hartree)
Re +0.000000 +0.000000 +0.000000
N +2.223480 +0.000000 +0.000000
N +0.206600 +0.000000 -2.198250
N +0.206580 -2.128040 -0.551120
N +4.278770 +0.462310 +0.597290
C +2.979660 +0.668730 +0.863980
C -1.927290 -0.068230 -0.088150
C -0.067420 -0.249820 +1.911490
C -0.067420 +1.913070 +0.237400
C +0.237940 +1.067180 -2.993280
C +0.378660 +0.966640 -4.381870
C +0.492120 -0.273870 -4.964590
C +0.467640 -1.423410 -4.152040
C +0.319420 -1.236180 -2.764150
C +0.319400 -2.365960 -1.889690
C +0.467630 -3.662570 -2.418900
C +0.492090 -4.737370 -1.509800
C +0.378620 -4.484280 -0.162810
C +0.237930 -3.165240 +0.282660
C +0.600740 -2.753080 -4.665970
C +0.600760 -3.826720 -3.834950
C +4.375920 -0.376770 -0.486780
C +3.094790 -0.660140 -0.852890
O -3.083600 -0.111850 -0.144510
O -0.095800 -0.426390 +3.056760
O -0.095800 +3.066030 +0.353610
H +0.148830 +2.031120 -2.515530
H +0.399190 +1.870530 -4.973270
H +0.399120 -5.283400 +0.563950
H +0.148810 -2.944410 +1.335590
H +0.710340 -2.881720 -5.734870
H +0.710360 -4.829230 -4.227460
H +0.605900 -0.377600 -6.035710
H +0.605860 -5.748280 -1.878750
H +5.048870 +0.861250 +1.112720
H +2.754160 -1.283150 -1.657810
H +2.620490 +1.288710 +1.664990
H +5.321250 -0.689960 -0.891410
```

Supplementary References

[1] D. A. Case, D. S. Cerutti, T. E. Cheatham, III, T. A. Darden, R. E. Duke, T. J. Giese, H. Gohlke, A. W. Goetz, D. Greene, N. Homeyer, S. Izadi, A. Kovalenko, T. S. Lee, S. LeGrand, P. Li, C. Lin, J. Liu, T. Luchko, R. Luo, D. Mermelstein, K. M. Merz, G. Monard, H. Nguyen, I. Omelyan, A. Onufriev, F. Pan, R. Qi, D. R. Roe, A. Roitberg, C. Sagui, C. L. Simmerling, W. M. Botello-Smith, J. Swails, R. C. Walker, J. Wang, R. M. Wolf, X. Wu, L. Xiao, D. M. York and P. A. Kollman, *AMBER 2017*, http://ambermd.org/, 2017.

[2] S. Kossmann and F. Neese, *J. Chem. Theory Comput.*, 2010, **6**, 2325–2338.

[3] F. Neese, *WIREs Comput. Mol. Sci.*, 2012, **2**, 73–78.

[4] T. Morishita, *J. Chem. Phys.*, 2003, **119**, 7075–7082.

[5] S. Miyamoto and P. A. Kollman, *J. Comput. Chem.*, 1992, **13**, 952–962.

[6] T. Darden, D. York and L. Pedersen, *J. Chem. Phys.*, 1993, **98**, 10089–10092.